Int J Adv Manuf Technol (2016) 87:2639–2651
DOI 10.1007/s00170-016-8664-7

ORIGINAL ARTICLE

Study on requirement of nickel electroplating in OFE copper-316L stainless steel brazed joints

Abhay Kumar[1] · P. Ganesh[1] · R. Kaul[1] · D. P. Yadav[1] · A. K. Karnewar[1] · K. N. Yedle[1] · R. K. Gupta[1] · M. K. Singh[1] · P. Ram Sankar[1] · V. K. Bhatnagar[1] · R. Sridhar[1] · S. C. Joshi[1] · L. M. Kukreja[1]

Received: 19 May 2015 / Accepted: 20 March 2016 / Published online: 1 April 2016

Abstract The paper describes an experimental study to evaluate the need of nickel electroplating on stainless steel part in vacuum brazed oxygen-free electronic (OFE) copper-type 316L stainless steel transition joints with silver copper eutectic braze filler metal (BVAg-8 of AWS A5.8). The results of the study demonstrated that nickel electroplating is not required to obtain hermetically sealed sound and strong OFE copper-316L stainless steel transition vacuum brazed joints. The only pre-treatment requirement for stainless steel part is simple ultrasonic cleaning, although pickling treatment has been found to have a favorable effect in improving its wettability for the braze filler metal. Brazed joints made with unplated stainless steel (SS) not only displayed (i) required level of hermeticity (helium leak rate $\leq 2 \times 10^{-10}$ mbar·l/s) and bakeablility at 523 K for ultra-high vacuum application and (ii) reasonably good tensile strength comparable to those made with Ni-plated SS, but also exhibited significantly suppressed extent of intergranular penetration of braze filler metal into copper. Important factors responsible for the development of sound OFE copper-316L stainless steel brazed joints with ultrasonically cleaned stainless steel part are excellent wettability of OFE copper which compensated for poor wettability of stainless steel surface and presence of hydrocarbon-free high vacuum environment during brazing.

Keywords Brazing · Copper · Stainless steel · Nickel · Electroplating

✉ R. Kaul
rkaul@rrcat.gov.in

[1] Raja Ramanna Centre for Advanced Technology, P.O.: CAT, Indore 452 013, India

1 Introduction

Complex design issues of components of modern-day particle accelerators present unique challenges in material selection. Oxygen-free electronic (OFE) copper (ASTM F68, UNS Number C 10100) and austenitic stainless steel (SS) type 316L find widespread applications in particle accelerators all over the world. OFE copper, due to its high electrical and thermal conductivity, is invariably chosen as material of construction of normal conducting accelerating structures like radio frequency (RF) cavities of linear accelerators and circular accelerators and RF quadrupoles [1, 2]. On the other hand, SS 316L, due to its low electrical conductivity, good mechanical strength, high Young's modulus, and low magnetic permeability, finds applications in the construction of components which are placed in the vicinity of magnets where the unique combination of low thickness, low electrical conductivity, and low magnetic permeability leads to a reduction in two important design constraints—(i) eddy current generation during ramp and (ii) the distortion of the magnetic field. Both the materials have low specific outgassing rates; therefore, they share the commonality of being ultra-high vacuum (UHV)-compatible materials.

On many occasions, these materials complement each other. OFE copper has low yield strength; therefore, the most prevalent method of sealing OFE copper structures is to use knife edge flanges made of austenitic SS along with OFE copper gaskets. The sealing mechanism is through plastic yielding of the gasket material at the line of contact with the knife edge of the flanges. On the other hand, some austenitic SS components, due to their poor thermal conductivity, are often required to be water-cooled to limit outgassing and to avoid high thermal stresses and distortions. In order to facilitate efficient heat removal, austenitic SS components are often joined to copper tubes for water circulation. Sometimes

copper pieces are also used to disperse the heat to a larger area before it reaches the austenitic SS surface. Therefore, the transition joint of copper and austenitic SS is an indispensable need of many particle accelerator components. Some of the components utilizing Cu-SS transition joints are normal conducting RF cavities of linear accelerators, radio frequency quadrupoles, vacuum chambers for high brilliance machines, photon absorbers, beam slits, beam dumps, profile transition chambers for insertion devices, pinhole assembly, staggered pair monitor, scraper and slit assembly for emittance monitoring, and Faraday cup for measuring the ion current [3].

Fusion welding is not a preferred technique for joining OFE copper to austenitic SS due to (i) large mismatch in their thermal conductivities (Cu, 391 W/m·K (297 K); AISI 316L SS, 16 W/m·K (297 K)) [4, 5], (ii) limited mutual solubility in each other, and (iii) intergranular penetration of copper into austenitic SS, a phenomenon popularly known as copper contamination cracking (CCC) [6]. Instead, brazing or solid state welding processes are preferred for joining dissimilar metals involving metallurgical incompatibility [7–10]. Vacuum brazing due to its versatility, ease, and availability in almost all particle accelerator laboratories is widely used for fabricating OFE copper-stainless steel transition joints [11].

Silver-copper eutectic (BVAg-8 of AWS A 5.8 [12], 72 Ag/28Cu; $T_M = 1052$ K) is a popular braze filler metal (BFM) for the above application. Wettability of the substrates by the BFM is considered as one of the most important factors influencing establishment of satisfactory brazed joints. In the case of copper-SS dissimilar couple, copper is characterized by excellent wettability while austenitic SS is known for its poor wettability for BVAg-8 alloy at the brazing temperature of about 1073 K. Poor wettability of the austenitic SS surface is attributed to tenacious Cr_2O_3 film present on its surface [13]. A widely employed approach to obtain satisfactory wettability of austenitic SS surfaces involves electroplating it with nickel [14] or copper [15], although there are reports of satisfactory brazing of austenitic SS without recourse to plating [13, 16]. In view of prevailing uncertainty regarding the exact requirement of electroplating of austenitic SS part, the present experimental study has been undertaken to compare microstructural and mechanical characteristics of OFE copper-316L SS transition brazed joints made with and without nickel electroplating. The prime motive for undertaking this study was derived from authors' recent experimental studies on niobium-316L stainless steel brazing for targeted application in superconducting RF cavities. In view of poor wettability of niobium surface [17], the first part of the study was performed with Ti-activated BFM, CuSil-ABA®, while mating SS surface was electroplated with nickel which also served as a diffusion barrier besides improving its wettability [18]. The resultant brazed joints, although hermetically sealed, carried well-distributed intermetallic particles in the ductile matrix. In the subsequent study, aimed at minimizing brittle intermetallic formation, Nb-316L SS brazing was performed with BVAg-8 as the BFM. The study yielded sound intermetallic-free transition joints, in spite of poor wetting ability of niobium surface for BVAg-8 BFM [19]. A major factor responsible for establishment of sound Nb-316L SS brazed joint was identified as excellent wettability of nickel-plated SS surface which compensated for poor wettability of niobium surface. The present work represents an extension of the above observation to a similar transition brazed joint, comprising of highly wettable OFE copper and poorly wettable 316L SS. The result of the study would provide important input to the practicing engineers, particularly involved in the design and fabrication of components of particle accelerators.

2 Experimental Procedure

The experimental study involved two sub-studies. The first sub-study was aimed at examining the wettability of SS and OFE copper specimens for BVAg-8 BFM, whereas the second sub-study involved OFE copper-316L SS brazing and characterization of resultant joints. In the first sub-study, a simplified wettability test (sessile drop test) was performed on SS specimens under three different surface conditions: (i) ultrasonically cleaned, (ii) pickled, and (iii) nickel-plated to compare their wettability for BVAg-8 BFM. Apart from above mentioned specimens, the wettability test also included a chemically cleaned OFE copper specimen. In this test, a small piece (diameter, 1.6 mm; length, ~4 mm) of BVAg-8 wire was placed vertically on SS surface and subjected to experimental brazing thermal cycle in an indigenously built hydrocarbon-free vacuum furnace at a pressure of 2×10^{-5} mbar. The experimental brazing thermal cycle was as follows: room temperature (RT), 523 K at 3 K/min; soaking at 523 K for 10 min; 523–823 K at 2 K/min; soaking at 823 K for 10 min, 823–1033 K at 3 K/min; soaking at 1033 K for 40 min; 1033–1073 K at 5 K/min; soaking at 1073 K for 1 min; and followed by furnace cooling to RT. At the brazing temperature, the partial pressures of oxygen and water vapor were recorded as 2×10^{-9} and 4×10^{-7} mbar, respectively. After cooling down to RT, the specimens were examined under an optical microscope for contact angle measurement [20]. The measured contact angles provide useful semi-quantitative comparison of wetting characteristics of different kinds of treated surfaces in absence of a dynamic drop shape analysis system.

Ultrasonic cleaning procedure adopted for the SS specimens was as follows: (i) ultrasonic cleaning in 5 % EXTRAN MA03™ phosphate-free solution (pH = 12) at 333 K for 10–15 min, (ii) rinsing in cold water and drying, and (iii) ultrasonic cleaning in 2-propanol at 333 K for 10 min, whereas the pickling treatment involved immersion of SS specimens at room temperature for 15 min in an aqueous solution of 3 % HF and 20 % HNO_3. On the other hand, the

procedure adopted for nickel electroplating on SS parts involved (i) ultrasonic cleaning in trichloroethylene for 20 min to remove oil, grease, and dust particles; (ii) soak cleaning in alkaline solution of NaOH (20 g/l), Na_2CO_3 (20 g/l), and Na_3PO_4 (32 g/l) for 20 min at 323–328 K; (iii) chemical cleaning for 15–20 min in a solution of HNO_3 (20 % *v*/*v*), and HF (2 %) at RT followed by 1-min anodic and cathodic cleaning in H_2SO_4 (20 % *v*/*v*) at a current density of 0.05 A/cm^2; (iv) nickel strike in chloride nickel bath ($NiCl_2$ and HCl) for 5 min at a current density of 0.05 A/cm^2; and (v) nickel deposition for 5 min in Watts' bath containing nickel sulfate, nickel chloride, and boric acid at a current density of 0.03 A/cm^2 at 323–328 K. The thickness of nickel plating was found to be 2–3 μm. The procedure adopted for chemical cleaning of copper substrate was as follows: (i) ultrasonic cleaning in trichloroethylene, (ii) immersion cleaning in 50 % HCl (*v*/*v*) for 3–5 min, (iii) rinsing with water, (iv) dipping in chromic acid solution (50 g/l chromic acid and 5 ml/l sulphuric acid) for 0.5–1 min, (v) rinsing with water, (vi) repeating steps (ii) to (v) two to three times depending on the cleanliness of the job after each stage, (vii) final cleaning in 10 % sulphuric acid (*v*/*v*) for 2–3 min, and followed by (viii) rinsing with tap water, DM water, and drying.

In the second experimental sub-study, vacuum brazed joints between OFE copper and type 316L SS were made in sandwich and capillary configurations using BVAg-8 BFM. The SS parts used for fabrication of brazed joints were given the same three different surface treatments, viz., (i) ultrasonically cleaning, (ii) pickling, and (iii) nickel plating. In the forthcoming text, the corresponding Cu-SS brazed specimens are referred as "ultrasonically cleaned," "pickled," and "Ni-plated" brazed specimens, respectively. The sandwich brazed specimens were used as tensile test specimens, while the specimens brazed in capillary configuration were utilized to determine joints' hermeticity by helium leak testing (HLT) and thermal cycle test and also for microstructural analysis. While designing braze specimens for capillary joints, due consideration was given for sealing its two ends for carrying out helium leak testing. Capillary joints were brazed with a 1.6-mm-diameter wire of BFM. Figure 1 presents dimensional details of the brazed specimens used for the experimental study for making capillary joints. Preparation of tensile test specimens involved brazing with a 50-μm-thick foil of BFM sandwiched between dissimilar mating surfaces, as shown in Fig. 2. In view of the large difference in the strength of the materials, the OFE copper part of the tensile test specimen was made relatively wider than its SS counterpart to ensure tensile fracture of the brazed specimen at the joint. The details of fixture used for brazing of tensile test specimens are provided in Fig. 3. For temperature measurement during vacuum brazing, Inconel-sheathed N type job thermocouples were inserted in thermowells provided in the brazing fixture as well as in the capillary brazing samples. The diameter of the thermowells

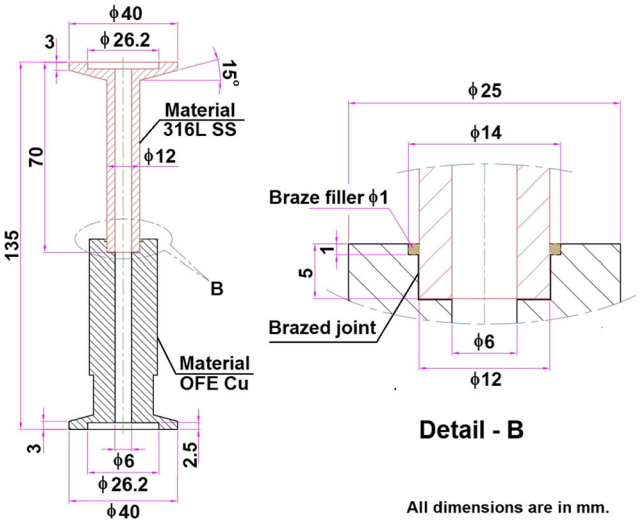

Fig. 1 Dimensional details of OFE Cu-316L stainless steel (tube–tube) pre-braze assembly for fabrication of specimen with capillary joint

was kept slightly bigger than the diameter of the sheathed thermocouple (3 mm) for easy insertion, and their depth was kept about five times the diameter.

The brazed specimens were characterized with respect to (i) microstructure and compositional details, (ii) tensile strength and associated fracture mode, and (iii) hermeticity using helium leak testing and bakeablility for ultra-high vacuum application. Microstructural characterization of vacuum brazed specimens was performed on capillary joints using optical and scanning electron microscope (SEM), integrated with energy-dispersive spectroscopy (EDS). HLT was conducted using Alcatel, ASM 182 TD+ leak detector. For helium leak testing, ISO-KF 25 interfaces provided at the two ends of the brazed assembly were sealed with FKM O-ring and the brazed assembly was directly mounted on the inlet port of leak detector. During HLT, hermeticity of the brazed joint was determined by spraying helium from outside the joint while the inside is evacuated to a pressure of 10^{-4} mbar.

3 Results

Visual examination of the three kinds of investigated surfaces of SS specimens of sessile drop test brought out significant difference in their ability to be wetted by BVAg8 BFM. Figure 4a compares shapes of melted and re-solidified pieces of BFM on (i) ultrasonically cleaned, (ii) pickled, and (iii) nickel-plated SS surfaces. Ultrasonically cleaned surface of SS specimen displayed obtuse contact angle of about 110°, thereby demonstrating its limited ability to be wetted by the BFM. Pickling treatment brought about a noticeable reduction in the contact angle from 110° to 47°, reflecting improvement in wetting character of the pickled surface with respect to ultrasonically cleaned surface. On the other hand, Fig. 4a, b

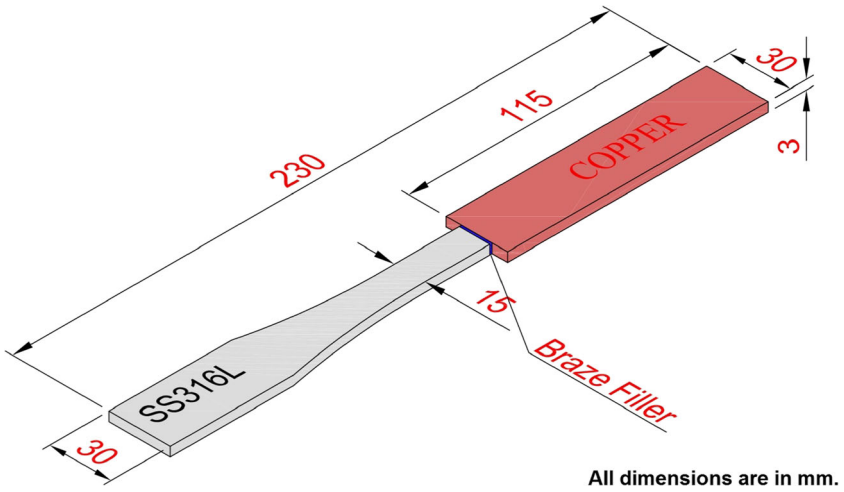

Fig. 2 Dimensional details of OFE Cu-316L stainless steel (sheet–sheet but joint) pre-braze assembly for fabrication of tensile specimen with butt joint

show excellent spreading of the BVAg8 BFM on the nickel-plated SS and OFE copper surfaces. This is indicative of very small wetting/contact angles in these cases. Metallographic examination of the cross section of unplated SS/BFM specimen displayed sharp interface with little noticeable diffusion across the interface. Figure 5 presents EDS concentration maps of Fe, Cr, Ni, Cu, and Ag across SS/BFM interface of the specimen (in sessile drop test) with ultrasonically cleaned SS substrate. In contrast, Ni-plated SS/BFM specimen revealed significant diffusion of copper, from BFM into nickel plating on the surface of SS part, as shown in Fig. 6a. Another noteworthy feature of the specimen was formation of Cu-rich cells in Ag-rich BFM, as marked with arrows in Fig. 6b. EDS spot measurements on some of the copper-rich cells confirmed presence of Ni (4.4–11.5) and Ag (2.6–4.5 %) (refer Fig. 6a). On the other hand, OFE copper/BFM specimen was marked with rippled interface between the two materials. EDS examination of the interfacial region displayed definite presence of Ag on the copper side of the specimen. Figure 7 shows the cross section of OFE copper/BFM in the sessile drop test specimen with associated EDS mapping and spot chemical composition in the copper substrate close to BFM.

Helium leak testing of three kinds of vacuum brazed Cu-SS assemblies (refer Fig. 1) at room temperature displayed no detectable leak against 7×10^{-11} mbar·l/s background of helium. Figure 8 shows helium leak–tested vacuum brazed assemblies, along with close-up views of the brazed regions. An important feature of Ni-plated vacuum brazed assembly was spread of BFM on unintentionally nickel-plated surface of SS part. On the other hand, ultrasonically cleaned and pickled brazed assemblies were marked with preferential spread of BFM on copper part. Helium leak tightness of the brazed joints remained intact after undergoing 5 numbers of thermal cycles, each involving heating to 523 K, soaking for 8 h, and then cooling to RT. This ensured bakeability of the brazed joints for UHV application.

Cross-sectional examination of the above three specimens exhibited complete braze penetration without any signature of

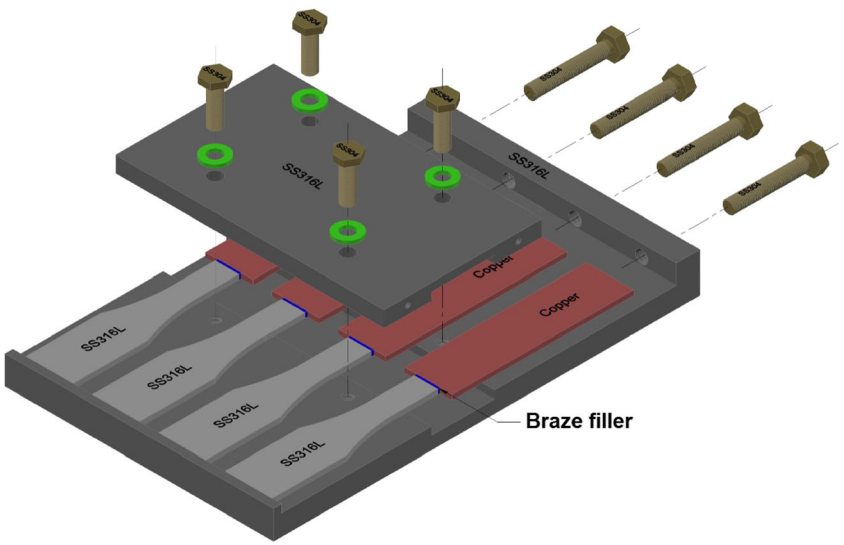

Fig. 3 Schematic exploded view of the fixture used for brazing OFE Cu-316L stainless steel tensile test specimens

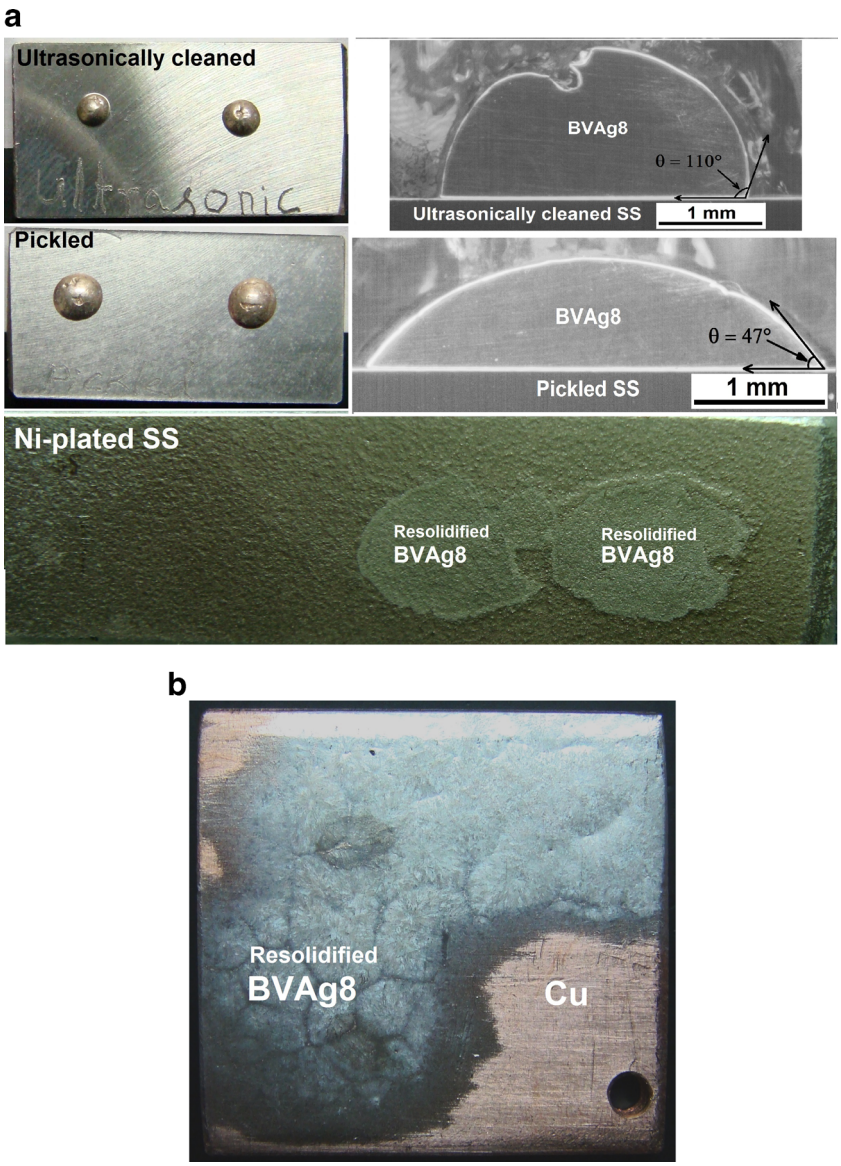

Fig. 4 **a** Comparison of the shapes of melted and re-solidified braze filler metal (BVAg8) on ultrasonically cleaned, pickled, and Ni-plated surfaces of stainless steel specimens in sessile drop test (θ, angle of wetting). Complete spreading of the BVAg8 braze filler on the nickel-plated SS is indicative of very small angle of wetting. **b** Resolidified layer of BVAg8 braze filler metal on OFE copper specimen in sessile drop test. Complete spreading of the BVAg8 braze filler on the OFE copper surface is indicative of very small angle of wetting

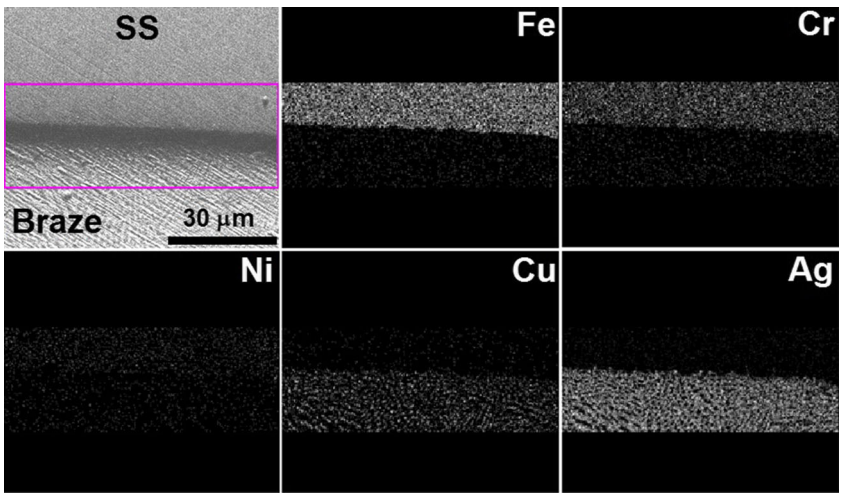

Fig. 5 Cross section of the ultrasonically cleaned SS/BFM interface of the specimen in sessile drop test and associated EDS compositional maps of Fe, Cr, Ni, Cu, and Ag. *Rectangle* represents the region used for EDS measurements

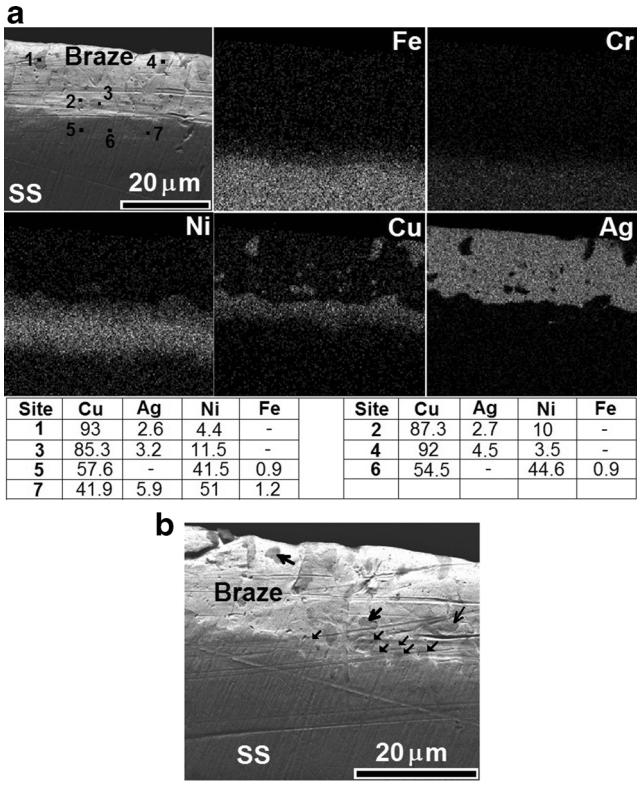

Site	Cu	Ag	Ni	Fe
1	93	2.6	4.4	-
3	85.3	3.2	11.5	-
5	57.6	-	41.5	0.9
7	41.9	5.9	51	1.2

Site	Cu	Ag	Ni	Fe
2	87.3	2.7	10	-
4	92	4.5	3.5	-
6	54.5	-	44.6	0.9

Fig. 6 **a** Cross section of the nickel-plated SS/ resolidified braze metal interface of the specimen (in sessile drop test) and associated EDS compositional maps of Fe, Cr, Ni, Cu, and Ag. The table at the bottom presents results of spot EDS measurements on sites marked in secondary electron image (*top left*). **b** Cross section of resolidified BVAg8 braze filler metal on nickel-plated 316L stainless steel (in sessile drop test) showing copper rich cells (marked with *arrows*) in the BFM

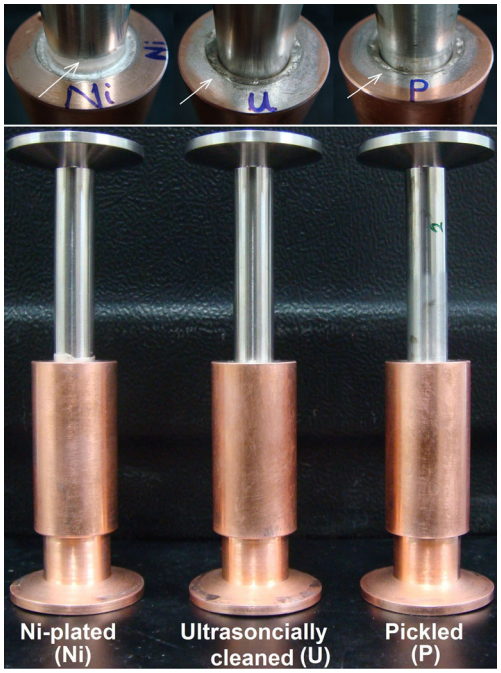

Fig. 8 Vacuum brazed and helium leak tested OFE Cu-316L stainless steel specimens. Inset at top shows magnified view of the brazed joint region; the spread of braze filler metal is marked with *arrows*

lack of bonding or porosity in the brazed joint. Figures 9, 10, and 11 present cross sections of ultrasonically cleaned, pickled, and Ni-plated brazed specimens, respectively. All the specimens displayed good bonding of the braze metal with the two substrates. Brazed joints of ultrasonically cleaned and pickled specimens exhibited typical eutectic microstructure, comprising of Ag-rich (bright) and copper-rich (dark) phases (refer to Figs. 9 and 10). There was no noticeable intergranular penetration of BFM into SS part. Sharp nature of SS/braze interface in these specimens is attributed to limited mutual solubility of copper and silver in iron. On the other hand, copper/braze interface was rippled in nature. Brazed joints in both ultrasonically cleaned and pickled specimens exhibited limited intergranular penetration of BFM into copper at sporadic places. Figure 11 shows extensive pullout of surface grains of copper in the case of Ni-plated brazed specimens. Figure 12a presents EDS concentration maps of Fe, Cr, Ni, Cu, and Ag across the cross section of brazed joint between OFE copper and ultrasonically cleaned SS. In this specimen, copper part of the brazed specimens recorded 4.2–6.6 % Ag, along with a small amount of Fe (0.3–0.4 %) in the region close to its interface with BFM, as shown in Fig. 12b. Presence of small amount of Fe in the interfacial region of copper, arising as a result of its diffusion (from SS part) across

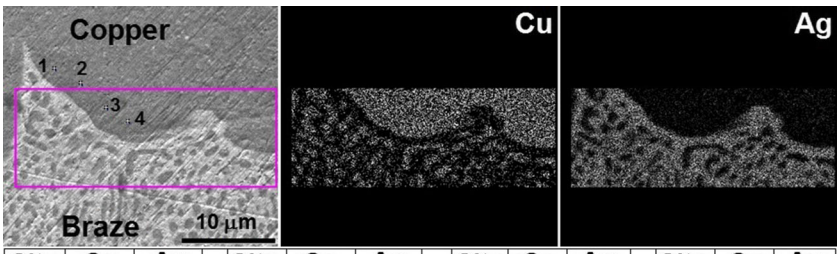

Site	Cu	Ag
1	81.3	18.7

Site	Cu	Ag
2	92.9	7.1

Site	Cu	Ag
3	96.2	3.8

Site	Cu	Ag
4	95.2	4.8

Fig. 7 Cross section of resolidified BVAg8 braze filler metal on OFE copper (in sessile drop test) and associated EDS compositional maps. *Rectangle* marks the region used for EDS measurements. The table at the bottom presents results of spot EDS measurements on sites marked in secondary electron image (*top left*)

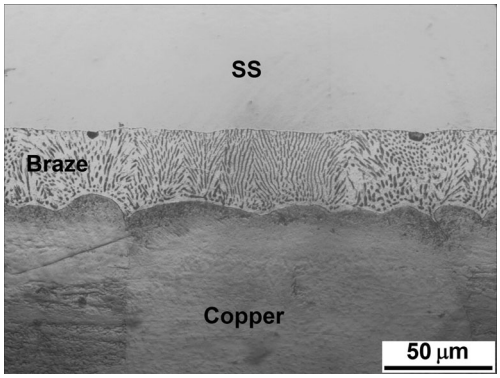

Fig. 9 Microstructure of the cross section of "ultrasonically cleaned" 316L SS and OFE Cu brazed specimen. The specimen displayed fine eutectic structure in the braze joint with limited intergranular penetration of BFM into copper substrate at sporadic places

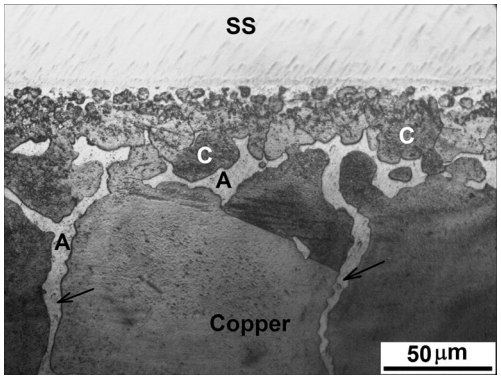

Fig. 11 Microstructure of the cross-section of "Ni-plated" 316L SS and OFE Cu brazed specimen showing excessive penetration of Ag-rich BFM (marked with *arrows*) into OFE copper substrate. *C*: pulled out (Cu,Ni,Ag) cells; *A*: Ag-rich BFM

the brazed joint, does indicate establishment of intimate contact between BFM and deoxidized surface of SS part. With respect to ultrasonically cleaned and pickled specimens, Ni-plated brazed specimen was characterized by significantly deeper penetration of BFM into copper grain boundaries (refer Fig. 11). BFM penetration in the copper grain boundary was found to be rich in silver, with copper content of 6.6–7.2 wt%, which is within the maximum solubility limit of Cu in Ag at 1052 K (8.8 wt%). Intergranular penetration of BFM was severe enough to result in complete "pullout" of Cu-rich grains in Ag-rich BFM. Figure 13 presents EDS concentration maps across OFE copper/Ni-plated SS brazed joint. The figure shows noticeable presence of Ni, along with Ag, Fe, and Cr in "pulled out" Cu-rich grains surrounded by Ag-rich BFM. These pulled out grains bridged the braze gap to make the brazed joint not easily distinguishable (refer to Figs. 11 and 13).

Tensile testing of all three kinds of brazed Cu-SS specimens exhibited comparable tensile strength values. Table 1 summarizes results of tensile tests. It should be noted that tensile fracture in ultrasonically cleaned and pickled brazed specimens was preceded by extensive plastic deformation (in the form of thinning) than the "Ni-plated specimens." In contrast to fracture of Ni-plated brazed specimens in the brazed joint, the site of fracture in ultrasonically cleaned and pickled brazed specimens was mostly at copper/braze interface and also partly in the braze, as shown in Fig. 14. Detailed fractographic examination of SS part of tensile tested specimen revealed coarse dimples signifying ductile mode of fracture in the braze metal. Figure 15 presents dimpled morphology of the fracture surface of tensile tested Ni-plated brazed specimen. On the other hand, tensile fracture surface (SS part) of ultrasonically cleaned specimen exhibited two distinctly different regions, viz., coarse dimpled and relatively flatter regions as shown in Fig. 16a. Higher-magnification examination of flatter regions displayed presence of significantly finer dimples, as shown in Fig. 16b. The coarse dimpled and fine dimpled (appear flat at low magnification) regions of the fracture surface represent fractures at Cu/braze and SS/braze interfaces, respectively. In the case of pickled brazed specimen, tensile fracture surface of SS part displayed two regions of widely different topography. One part of the fracture surface was marked with coarse dimples while the other part displayed copper-rich grains protruding out of re-solidified film of BFM, as shown in Fig. 17. The coarse dimpled fracture represents fracture in eutectic BFM while latter feature is produced as a result of intergranular fracture in BFM penetrated into the grain boundaries of OFE copper (refer Fig. 14).

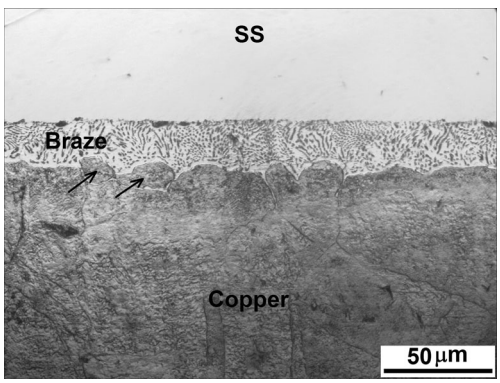

Fig. 10 Microstructure of the cross-section of "pickled" 316L SS and OFE Cu brazed specimen with eutectic structure in the braze joint. Copper-braze interface was associated with "pulled out" copper grains at some locations which is marked with *arrows*. Etchant: 50 % nitric acid and 50 % acetic acid (for copper)

4 Discussion

Wetting of mating metallic surfaces by molten BFM is the most important parameter influencing brazeability of a given joint. Wetting ability of a surface by molten BFM is primarily determined by stability of its oxide surface film. In the case of SS, reduction of tenacious surface film of chromium oxide at the brazing temperature is essential for establishment of sound

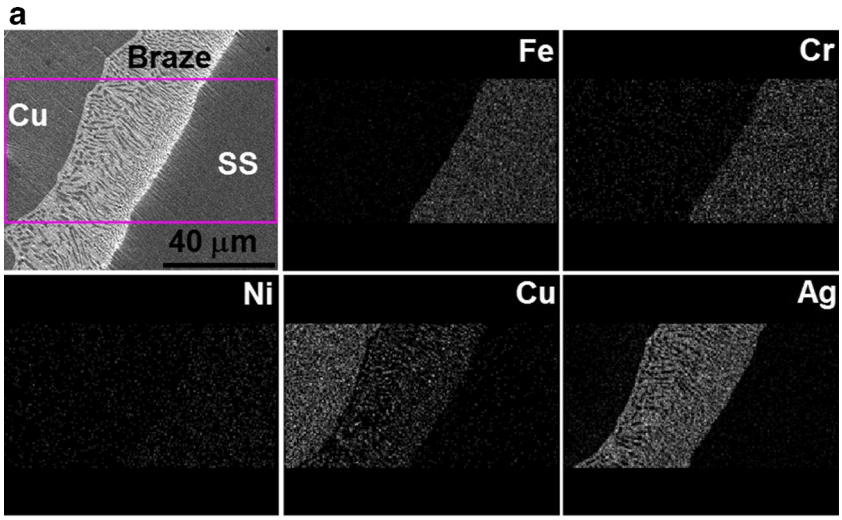

Site	Cu	Ag	Fe	Site	Cu	Ag	Fe
1	94	5.7	0.3	2	93.3	6.3	0.4
3	95.5	4.2	0.3	4	93.1	6.6	0.3

Fig. 12 **a** Microstructure of the cross section of "ultrasonically cleaned" 316L stainless steel and OFE Cu brazed specimen and associated EDS compositional maps. *Rectangle* marks the region used for EDS measurements for elemental mapping. **b** Microstructure of the cross section of "ultrasonically cleaned" 316L SS and OFE Cu brazed specimen and results of EDS spot analysis performed on sites marked in the figure

brazed joint. Keller et al. reported poor wettability index of unplated type 304L, 316L, and 21-6-9 SS for BFM BAg8 in the temperature range of 1073–1223 K [20]. With respect to chromium oxide, oxides of nickel and copper are considerably easier to get reduced. According to Ellingham diagram, the temperature required for reduction of surface oxides of copper and nickel at oxygen partial pressure of 10^{-9} mbar (while considering oxide reduction under existing level of oxygen partial pressure in the vacuum furnace) is about 660 and 875 °C, respectively [21]. In contrast, chromium oxide film present on the surface of SS part is not likely to get reduced below the melting temperature of underlying substrate (refer Fig. 15). It should be noted that actual reduction temperature of surface oxides will be also be determined by level of pCO/pCO_2 and pH_2/pH_2O in the furnace atmosphere. Hence, electroplating SS mating surface with copper and nickel provides a wettable oxide-free surface at the brazing temperature of about 1073 K. This is validated by significantly higher contact angle of BVAg-8 BFM on unplated SS surface than those observed on copper and nickel-plated surfaces.

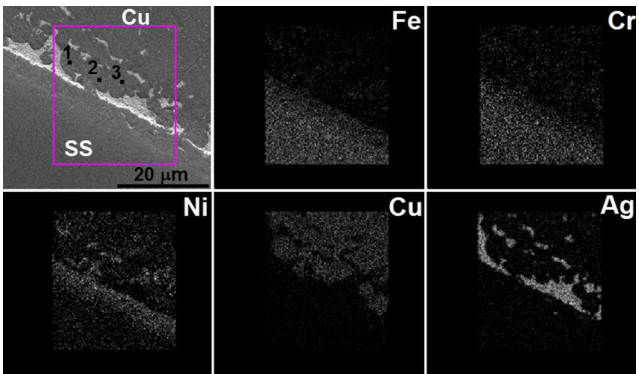

Site	Cu	Ni	Fe	Ag	Site	Cu	Ni	Fe	Cr	Site	Cu	Ni	Fe	Ag
1	87.5	8.4	1.9	2.2	2	72.5	17.8	7.8	1.9	3	87.5	8.7	1.7	2.1

Fig. 13 SEM image of the cross section of "Ni-plated" 316L SS and OFE Cu braze joint and associated EDS compositional maps. *Rectangle* marks the region used for EDS measurements for elemental mapping. The table at the bottom summarizes results of spot EDS measurements on sites marked in secondary electron image (*top left*)

On the basis of above discussion, it is evident that during heating of OFE copper substrate in contact with BVAg-8 BFM, copper surface is deoxidized well below the melting temperature of BFM. Cleaned metallic surface available at the brazing temperature facilitates excellent spreading of BFM. The results of SEM-EDS examination suggests that at copper/BFM interface, non-planar growth of (Cu,Ag) phase occurs as a result of Ag diffusion from molten BFM into copper (along with Cu diffusion into BFM in which it is partitioned into Cu-rich phase of solidified BFM; refer to Fig. 7). It should be noted that due to limited solubility of silver in copper (7.9 % at 1051 K), the growth of (Cu,Ag)

Table 1 Results of tensile tests on vacuum brazed Cu-316L stainless steel specimens

Pre-treatment of SS part	Tensile strength (MPa)	Failure site
Ultrasonically cleaned	172–200	Partly in braze; partly at Cu/braze interface
Pickled	159–182	Copper/braze interface
Ni-plated	163–181	Brazed joint

phase is likely to be slower, although relatively faster diffusion of silver occurs along copper grain boundaries. Nickel-plated surface in contact with molten BFM displays non-planar growth of (Cu,Ni,Ag) ternary cells into the melt [22]. Growth of (Cu,Ni,Ag) cells involves diffusion of Cu and Ag into Ni electroplated layer (along with limited Ni diffusion into BFM due to its very low solubility in BFM). This is reflected in high concentration of Cu in Ni-plated layer (refer Fig. 6a). Because of unlimited mutual solid solubility of Cu and Ni, growth of (Cu,Ni,Ag) phase occurs rapidly and results in strong Cu depletion in BFM. This is followed by rapid Ag diffusion through (Cu,Ni,Ag) cells leading to complete pull-out of (Cu,Ni,Ag) ternary cells into Ag-rich BFM (refer Fig. 6b). In the case of brazing of Ni-plated SS with OFE copper part, brazing involved (i) rapid diffusion of copper and silver (from BFM) into nickel plating, (ii) diffusion of Ag into OFE copper grains and grain boundaries, and (iii) transport of Ni (from plating) through molten BFM and diffusion into Cu grains (possessing unlimited solid solubility for Ni). These three effects culminated into complete pullout of (Cu,Ni,Ag) cells and grains into Ag-rich BFM (refer Fig. 11). In a recent study reported by Fukikoshi et al., considerable intergranular penetration of molten BAg8 into copper was also observed in copper-304 SS brazed joint [16]. Authors attributed this effect to dissolution of Ni from the SS into the molten BFM. Xin et al. also demonstrated that during brazing of oxygen-free copper to Ni-containing base metal, nickel element rapidly dissolves in the BFM and leads to intergranular penetration into copper [23].

On the other hand, simplified wettability test on ultrasonically SS specimens displayed its limited wettability for molten BVAg-8 BFM. Due to limited mutual solubility of major constituents of SS and BFM, SS/BFM interface was quite sharp and it did not exhibit noticeable dilution across this interface (refer Fig. 5). Poor wettability of the ultrasonically cleaned SS surface for BVAg-8 does not explain full infiltration of BFM into the capillary joints which are more sensitive to wettability of the surface as compared to sandwich brazing [24]. It may be noted that in the present case, the brazed joint was formed between two dissimilar surfaces (SS and copper), with widely different wetting characteristics. In contrast to SS, copper surface is known for its excellent wettability for BVAg-8 [13, 25] which has also been confirmed by the wettability experiment. In this type of joint, wetting of both the surfaces by the molten BFM must be taken into account. The criterion for spontaneous ingress of BFM into the capillary is $\theta_{copper} + \theta_{316L} < 180°$ [24]. Therefore, it can be inferred that poor wettability of the SS surface was adequately compensated by excellent wettability of the copper surface, thereby facilitating spontaneous ingress of BFM BVAg-8 into the capillary gap. In a recent study on vacuum brazing of niobium to nickel-plated type 316L SS performed in authors' laboratory, satisfactory capillary brazed joints were obtained with BVAg-8 BFM, in spite of poor wettability of niobium surface [19]. After spread of BFM into the capillary gap, establishment of bonding between SS and BFM would be determined by the presence of surface oxide film (if any) on the SS part.

In early 1940s, Holm et al. [26, 27] proposed that during heating in vacuum (temperature = approximately 1323 K), chromium oxide film on 18/8 SS surface is reduced through its following reaction with carbon present in the specimen: $Cr_2O_3 + 3C \rightarrow 2Cr + 3CO$. In a related study conducted by Yoshiaki et al. [28], a striking increase in CO gas in vacuum chamber was cited as a supporting evidence in favor of

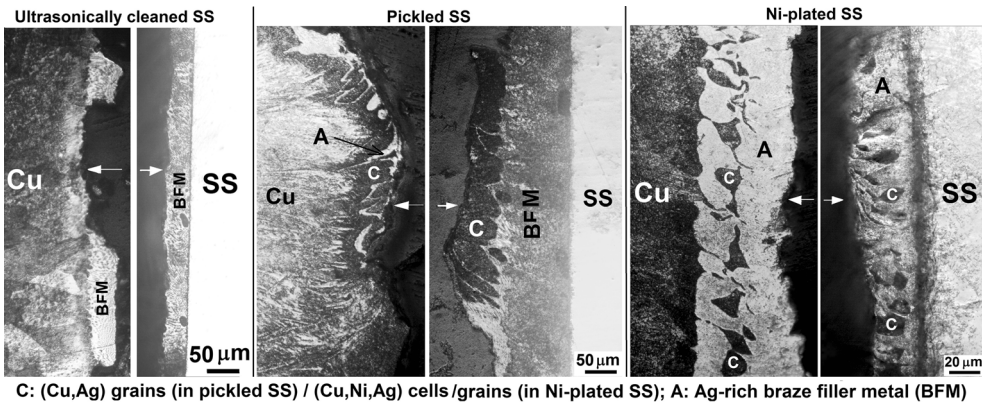

Fig. 14 Cross sections of mating fracture surfaces of tensile tested "ultrasonically cleaned," "pickled," and "Ni-plated" 316L stainless steel and OFE Cu brazed specimens. Fracture edges are marked with *arrows*. *A*: silver rich phase; *C*: copper rich phase; etchant: 50 % nitric acid and 50 % acetic acid (for copper)

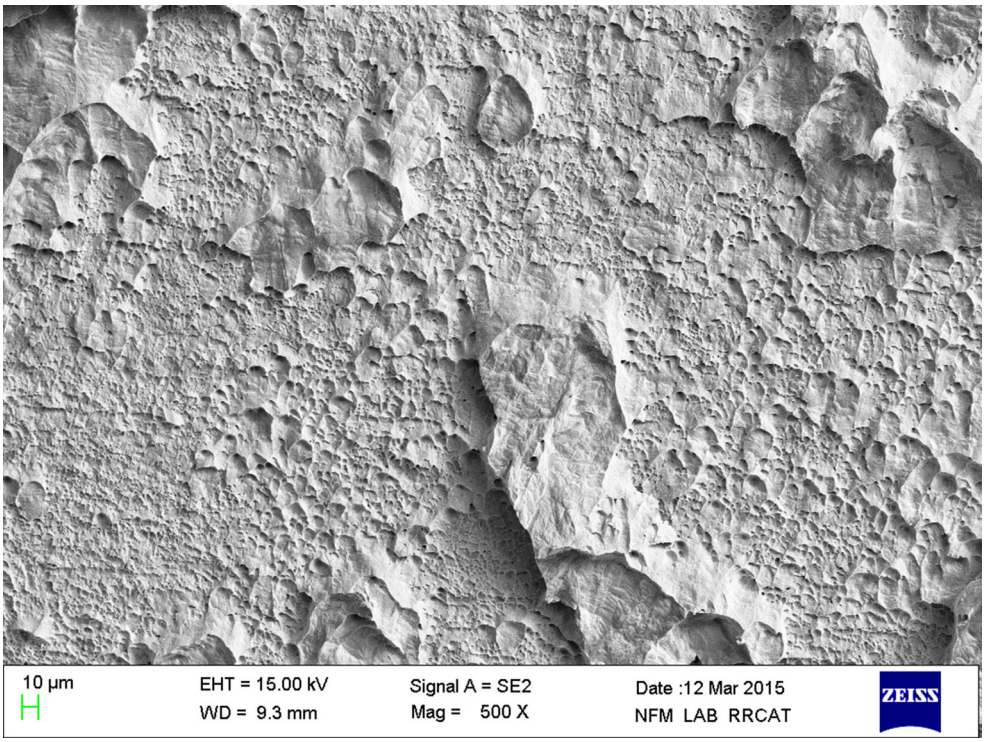

Fig. 15 Dimpled morphology of tensile fracture surface of "Ni-plated" 316L stainless steel and OFE Cu brazed specimen. Site of fracture was in the braze joint

proposed carbo-thermic reduction of chromium oxide surface film. Authors reported that reduction of chromium oxide surface film on 304L SS specimen is initiated at 1053 K at the grain boundaries of the SS substrate, forming grooves in oxide film which facilitates intergranular penetration of molten BFM into SS. At 1133 K, surface oxide film is completely removed. The above theory of carbo-thermic reduction of chromium oxide film present on the surface SS has also been accepted by Kozlova et al. [13]. In this paper, authors demonstrated that wetting of SS by Cu-Ag eutectic in high vacuum at a temperature of 1073–1173 K involves two reactive spreading stages—the first stage marked with abrupt drop in contact angle (θ) from about 130° to 30°–60° is controlled by steel deoxidation while the subsequent stage, involving dissolutive wetting, causes further reduction in θ by 10°–30°. The chemistry of the surface of SS part is solely determined by the duration of its exposure at a given temperature and not by duration of its contact with molten BFM BVAg-8. For type 321 SS, onset of surface deoxidation at a temperature of 1093 K (furnace pressure = 2×10^{-5} Pa) was observed after 1.5 min and complete surface deoxidation was recorded in 15 min. On the other hand, type 316L SS has been shown to

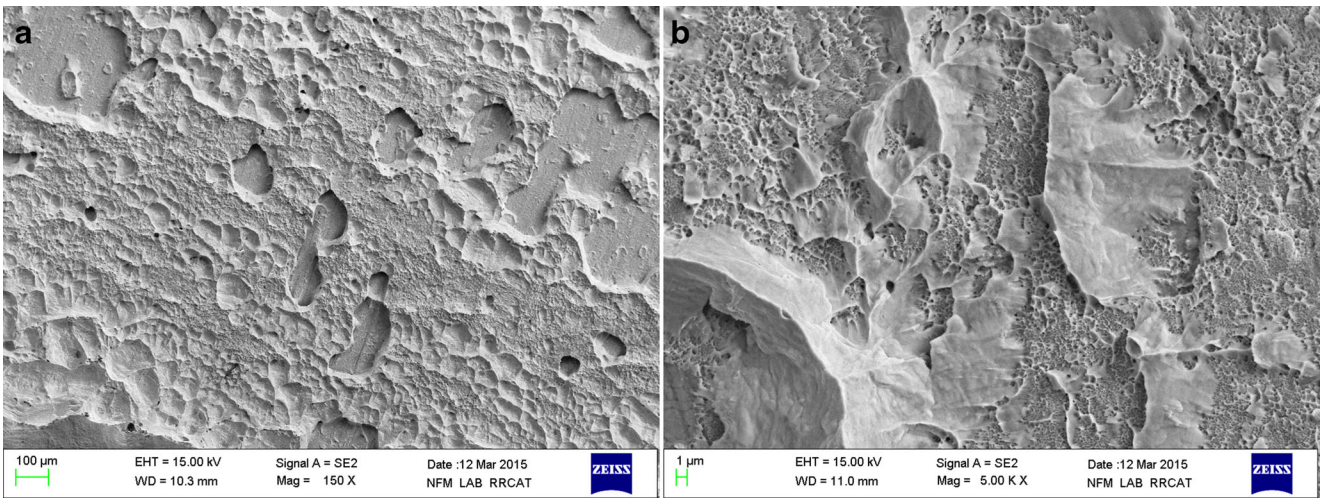

Fig. 16 Fracture surface of tensile tested "ultrasonically cleaned" 316L stainless steel and OFE Cu brazed specimen. **a** Coarse dimples and relatively flatter regions, **b** magnified view of flat regions showing significantly finer dimples

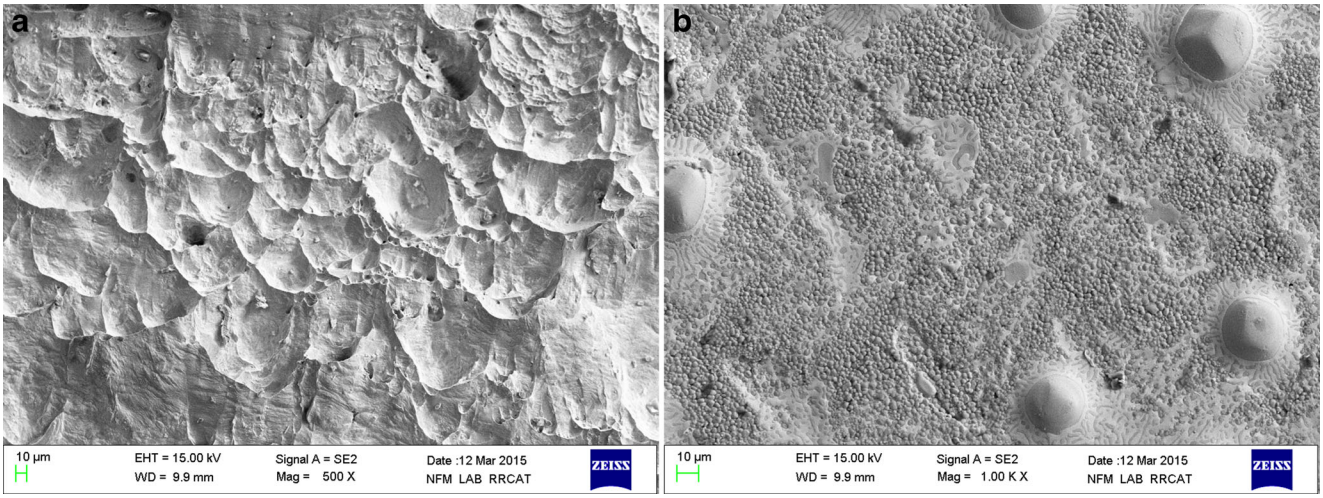

Fig. 17 Fracture surface of tensile tested "pickled" 316L stainless steel and OFE Cu brazed specimen. **a** Coarse dimples and **b** part of the fracture surface showing copper grains protruding out of re-solidified layer of braze filler metal

be wetted at lower temperatures with its contact angle several tens of degrees lower than that of type 321 SS. In the light of the above reports, it is believed that surface deoxidation of type 316L SS specimens took place under the experimental conditions such as operating pressure of 2×10^{-5} mbar, low partial pressures of oxygen and water vapor, a large soaking time at 1033 K, and a slower heating rate from melting temperature (1052 K) to brazing temperature (1073 K) than reported by Kozlova et al. [13]. Deoxidation of SS surface would facilitate diffusion across SS/BFM interface to establish bonding [29]. The improvement in wettability of SS surface caused by pickling (refer Fig. 4a) is attributed to formation of grain boundary grooves, as shown in Fig. 18. Similar results are also reported by Yoshiaki et al. [28]. Oxide film formed in the pickling induced groove region is likely to experience greater stress concentration generated due to mismatch in the coefficients of expansion between SS substrate (16×10^{-6}/K) [5] and chromium oxide film ($5.86–8.12 \times 10^{-6}$/K) [30] during specimen's exposure to elevated temperature [31–34]. This will eventually lead to rupture of the oxide film, thereby facilitating wetting of SS surface with molten BFM. On the basis of metallographic analysis of brazed joints, it is firmly demonstrated that the vacuum brazed joints of OFE copper with ultrasonically cleaned and pickled SS parts were not only sound but also microstructurally superior (in terms of intergranular penetration of BFM into OFE copper) to those made with Ni-plated SS. During tensile testing of OFE copper/316L SS brazed specimen, the resultant plastic deformation is concentrated at the brazed region due to its significantly (i) lower yield strength with respect to 316L SS and (ii) higher magnitude of imposed tensile stress with respect to OFE copper part of much larger ligament area (refer Fig. 2). Some scatter in the brazed joint thickness cannot be avoided in spite of making the tensile test joints using the same fixture. In the composite specimen, deformation of brazed joint is resisted by restraints imposed by its two surrounding substrates. The thinner the brazed joint, the greater will be the associated restraining effect which will be reflected in its higher strength [35, 36], and this is a major contributing factor in the scatter seen in the tensile strength of the brazed specimens. In the present case, restraint experienced by the brazed joint arises from (i) higher yield strength of SS part and (ii) lower tensile stress on Cu part (due to its considerably greater ligament area). Although all the specimens were assembled and brazed in the same fixture, there could be slight variation in the applied pressure at the interface of copper and SS parts of the tensile specimen, which may result in slight variation in the braze joint thickness. The brazed joint of ultrasonically cleaned specimen, due to its finely distributed eutectic microstructure, deforms as a single entity. However, any grain pull-out of copper surface grains will locally produce duplex microstructure of blocky (Cu,Ag) grains dispersed in softer Ag-

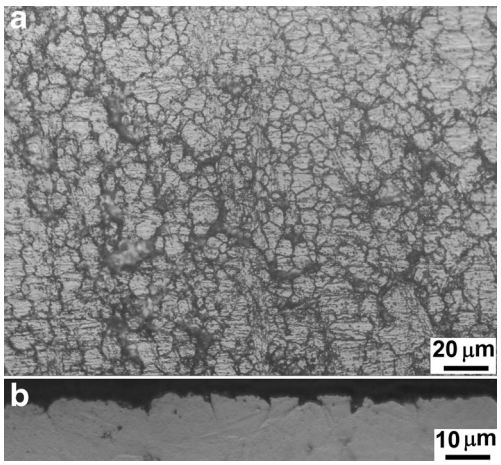

Fig. 18 Microstructure of **a** surface and **b** cross section of pickled 316L stainless steel specimen showing grain boundary grooves on the pickled surface

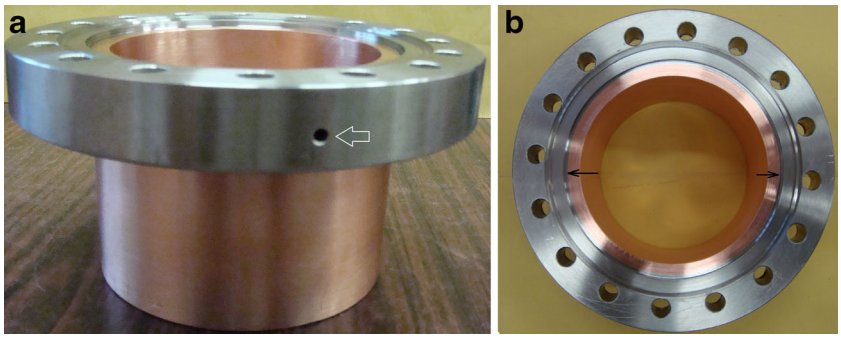

Fig. 19 Photographs of **a** side and **b** top views of vacuum brazed OFE Cu tube-316L SS flange port assembly. *Arrow* marks one of the "thermowells" provided for placement of thermocouple (**a**) and location of the braze joint along the circumference (**b**)

rich matrix close to Cu/BFM interface. In such a condition, plastic deformation would tend to occur in a thin layer of relatively softer Ag-rich BFM at Cu/BFM interface. This promotes failure of such specimens either in the BFM or at Cu/BFM interface. In contrast, Ni-plated brazed specimens were characterized by large-scale pull-out of blocky (Cu,Ni,Ag) grains/cells (from both nickel plating as well as copper substrate) uniformly distributed in softer Ag-rich BFM throughout the brazed joint. It may be noted that nickel is one of the commonly used solid solution hardening elements for copper [37]. Addition of nickel to copper significantly increases its strength (tensile and fatigue strength) [38]. During tensile testing of such specimens, relatively softer Ag-rich part of BFM would tend to preferentially deform with respect to harder blocky (Cu,Ni,Ag) grains/cells, leading to fracture in BFM.

Although all three kinds of brazed joints, made with ultrasonically cleaned, pickled, and Ni-plated SS parts displayed (i) required level of helium leak rate and (ii) fairly good tensile strength with ductile mode of fracture, significantly reduced extent of dissolution of copper base metal in ultrasonically cleaned and pickled brazed joints provides them a clear advantage over those made with Ni-plating of SS part.

In order to firmly establish "non-requirement" of nickel plating for obtaining a sound brazed component, a typical vacuum port joint, involving vacuum brazing of OFE copper pipe (DN90 SCH 40) to 316L SS flange (Type - 6 in. OD as per ASTM E2734/E2734M - 10 [12] (pre-braze radial gap = 40 μm; length of capillary joint = 17 mm) was fabricated without recourse to nickel plating. The SS flange was subjected to ultrasonic cleaning before assembling it with copper tube for subsequent brazing operation. Brazing was performed with 1.6-mm-diameter wire of BVAg8 BFM, placed in the groove provided in SS flange. Cleaning and brazing parameters were the same as described above. Figure 19 shows the photographs of vacuum brazed component. The brazed component not only exhibited desired level of hermeticity (helium leak rate better than 2×10^{-10} mbar·l/s) but also sustained 5 simulated baking cycles (each involving heating from RT to 523 K at 50 K/h, soaking at 523 K for 8 h, followed by cooling down to RT) without experiencing any deterioration in helium leak rate, thereby demonstrating suitability of the brazed joint for service in UHV condition.

5 Conclusions

In the light of the results of the study, it is demonstrated that for vacuum brazing of OFE copper-316L SS transition joints with BVAg-8 braze filler, SS part is not required to be electroplated with nickel, provided a clean vacuum environment is maintained during the course of brazing operation. Simple ultrasonic cleaning of SS part in suitable organic solvents (EXTRAN MA03 phosphate-free solution and 2-propanol in the present case) is enough to yield sound transition joints, although pickling treatment of SS part does improve its wetting ability for the braze filler metal BVAg-8. Brazed joints made with unplated SS not only displayed (i) required level of hermeticity and bakeablility for ultra-high vacuum application and (ii) good tensile strength comparable to those made with Ni-plated SS but also exhibited significantly suppressed extent of intergranular penetration of braze filler metal into copper. Major contributing factors for establishment of sound brazed joints include excellent wettability of OFE copper which compensates for poor wettability of SS surface and clean vacuum environment during brazing.

Acknowledgments Authors thankfully acknowledge UGC-DAE-CSR, Indore, Corporate R & D, Bharat Heavy Electricals (BHEL) Ltd., Hyderabad, and Advanced Materials and Processes Research Institute (AMPRI), Bhopal, for providing SEM-EDS facility for characterization of the specimens. They express their sincere thanks to Mr. V. K. Ahire of UGC-DAE-CSR, Mr. A. H. V. Pawan of BHEL, Hyderabad, and Mr. Anup Khare of AMPRI, Bhopal, for conducting EDS analysis of the brazed specimens. Authors thank Mr. A. P. Singh, Mr. C. Manikandan and Mr. G. S. Deshmukh for their useful contribution in chemical cleaning and nickel electroplating. They thank Mr. S. Sarkar for conducting helium leak testing of brazed specimens. Authors thankfully acknowledge technical assistance of Mr. Mukesh Chand, Mr. N. S. Yadav, Mr. Chinna Rao, Mr. S. K. Chourasia, Mr. J. S. Pulickal, Mr. Vedpal, Mr. Om Prakash, Mr. A. Chowdhury, and Mr. Ram Nihal Ram during various stages of the investigation. Authors also thank Mr. J. D. Zolpara for preparing drawings of test specimens and fixtures.

References

1. Gold SH, Ting A, Jabotinski V, Zhou B, Sprangle P (2013) Development of a high average current rf linac thermionic injector. Phys Rev ST Accel Beams 16:083401 (1–12)
2. Kondo Y, Morishita T, Hasegawa K, Chishiro E, Hirano K, Hori T, Oguri H, Sato F, Shinozaki S, Sugimura T, Kawamata H, Naito F, Fukui Y, Futatsukawa K, Nanmo K (2013) High-power test and thermal characteristics of a new radio-frequency quadrupole cavity for the Japan Proton Accelerator Research, Complex Linac. Phys Rev ST Accel Beams 16:040102 (1–8)
3. Tamura K, Oishi M, Ohkuma H, Okayasu Y, Shoji M, Takano S, Taniuchi Y, Masaki M, Mochihashi A (2013) Development of a high-heat-load compact photon absorber for SPring-8 diagnostics beamline II. J Phys Conf Ser 425(2013):212005. doi:10.1088/1742-6596/425/21/212005, 1-4
4. Cverna F (ed) (2012) Thermal properties of metals, ASM Ready Reference. ASM International, Materials Park, Ohio, p 410, 363
5. Li Y, Lin X, Vacuum Science and Technology for Accelerator Vacuum System. https//uspas.fnal.gov/materials/13Duke/USPASVacuumSession4_1VacMaterials.pdf. Accessed on 18 April 2015
6. Savage WF, Nippes EP, Mushala MC (1978) Copper-contamination cracking in the weld heat-affected zone. Weld J 57:145s–152s
7. Kore SD, Date PP, Kulkarni SV, Kumar S, Rani D, Kulkarni MR, Desai SV, Rajawat RK, Nagesh KV, Chakravarty DP (2011) Application of electromagnetic impact technique for welding copper-to-stainless steel sheets. Int J Adv Manuf Technol 54:949–955
8. Al-Roubaiy AO, Nabat SM, Batako ADL (2014) Experimental and theoretical analysis of friction stir welding of Al-Cu joints. Int J Adv Manuf Technol 71:1631–1642
9. Teker T (2013) Joining of stainless-steel and aluminum materials by friction welding. Int J Adv Manuf Technol 66:303–310
10. Zhu Z, Lee KY, Wang X (2012) Ultrasonic welding of dissimilar metals AA6061 and Ti6Al4V. Int J Adv Manuf Technol 59:569–574
11. Mathot S (2008) RFQ Vacuum Brazing at CERN, Proc. 11th European Particle Accelerator Conf. 2008. European Physical Society Accelerator Group (EPS-AG), Genoa, Italy, 1494–96
12. ASTM E2734/E2734M-10 (2010) Standard Specification for Dimensions of Knife-Edge Flanges. ASTM International, West Conshohocken
13. Kozlova O, Voytovych R, Devismes MF, Eustathopoulos N (2008) Wetting and brazing of stainless steels by copper-sliver eutectic. Mater Sci Eng A 495:96–101
14. Shaprio AE (2013) Brazing Q & A. Weld J 92:26
15. Singh R, Pant KK, Lal S, Yadav DP, Garg SR, Raghuvanshi VK, Mundra G (2012) Vacuum brazing of accelerator components. J Phys Conf Ser 390:012025
16. Fukikoshi T, Watanabe Y, Miyazawa Y, Kanasaki F (2014) Brazing of copper to stainless steel with a low-silver-content brazing filler metal, IOP Conference Series. Mater Sci Eng 61:012016
17. Liaw DW, Shiue RK (2005) Brazing of Ti-6Al-4V and niobium using three silver-base braze alloys. Metall Mater Trans 36A: 2415–2427
18. Kumar A, Ganesh P, Kaul R, Bhatnagar VK, Yedle K, Ram Sankar P, Sindal BK, Kumar KVANPS, Singh MK, Rai SK, Bose A, Veerbhadraiah T, Ramteke S, Sridhar R, Mundra G, Joshi SC, Kukreja LM (2015) A new vacuum brazing route for niobium-316L stainless steel transition joints for superconducting RF cavities. J Mater Eng Perform 24:952–963
19. Kumar A, Ganesh P, Kaul R, Sindal BK, Yedle K, Bhatnagar VK, Ram Sankar P, Singh MK, Rai SK, Bose A, Sridhar R, Joshi SC, Kukreja LM (2015) New brazing recipe for ductile niobium-316L stainless steel joints. Weld J. 94:241s–249s
20. Keller DL, McDonald MM, Heiple CR, Johns WL, Hofmann WE (1990) Wettability of brazing filler metals. Weld J 69:31–34
21. http://www.industrialheating.com/articles/89702-the-ellingham-diagram-how-to-use-it-in-heat-treat-process-atmosphere-troubleshooting, Accessed on 9 Oct. 2015
22. Zhuang WD, Eagar TW (1997) Diffusional breakdown of nickel protective coatings on copper substrate in silver-copper eutectic melts. Metall Mater Trans A 28A:969–977
23. Xin L, Wenqing Q, Haitao L, Guojian W (2014) Grain boundary penetration behavior analysis of OFC brazed with AgCu28 brazing filler. J Beijing University Aeronaut Astronaut 40:717–720
24. Sekulić DP (ed) (2013) Advances in Brazing - Science, Technology and Applications. Woodhead Publishing Ltd., Philadelphia, pp 3–28
25. Sharps PR, Tomsia AP, Pask JA (1980) Wetting and spreading in the Cu-Ag system., Lawrence Berkeley Laboratory, University of California. LBL-11119c.2. http://escholarship.org/uc/item/46c2n06b#page-1. Accessed on 20 April 2015
26. Holm VCF (1941) Observations on the tarnishing of stainless steels on heating in vacuum, Surface Treatment of Metals. American Society for Metals, Ohio, p 379
27. Holm VCF (1942) Elimination of oxide films on ferrous materials by heating in vacuum. J Res Natl Bur Stand 28:569–579
28. Yoshiaki A, Akira O, Fu CH (1983) Studies on vacuum brazing (Report II): removal of oxide film from stainless steel surface and brazing alloy spreading mechanism. Trans JWRI 12:27–34
29. Tweeddale JG (2013) The fabrication of materials: materials technology. Elsevier, London, p 129
30. Kirchner HP (1964) The thermal expansion of ceramic crystals. Prog Solid State Chem 1:1–36. doi:10.1016/0079-6786(64)90002-0-17
31. http://www.brazingandsoldering.org/faqs/faq7.pdf. Accessed on 20 March 2015
32. Philip R (2013) Industrial brazing practice, CRC Press, 2nd edn. Taylor and Francis Group, BocaRaton, p 221
33. Battenbough AJ, Osmanda Dipl.-Ing AM, Staines AM (2011) Surface preparation for high vacuum brazing., NICROBRAZ NEWS. www.wallcolmonoy.com/wp-content/uploads/ 2012/12/NicrobrazNews_Nov2011.pdf. Accessed 20 March 2015
34. Dorn L, Iversen K, Stroiczek M, Tillmann W, Weise W (2007) Hartloeten und Hochtemperaturloeten - Grundlagen und Anwendung. Expert Verlag, Renningen, Kontakt and Studium Band 677
35. Dan Kay. The famous joint-strength vs. joint clearance chart. http://vacaero.com/information-resources/vacuum-brazing-with-dan-kay/1300-the-famous-joint-strength-vs-joint-clearance-chart.html, Accessed on 9 Oct., 2015
36. M. H. Sloboda. Design and strength of brazed joints. http://www.jm-metaljoining.com/french/pdfs-uploaded/Design%20and%20Strength.pdf, Accessed on 9 Oct., 2015
37. ASM Specialty Handbook: Copper and Copper Alloys. Ed. J. R. Davis. ASM International, Materials Park, OH, 65.
38. Elements of Metallurgy and Engineering Alloys, Ed. F. C. Campbell, 2008, ASM International, Materials Park, OH, 482.